JOURNAL OF AGRICULTURAL AND FOOD CHEMISTRY
ARTICLE

J. Agric. Food Chem. 2009, 57, 7125–7130 7125
DOI:10.1021/jf9016306

Delivery of Bioactive Conjugated Linoleic Acid with Self-Assembled Amylose−CLA Complex

YING YANG, ZHENGBIAO GU, AND GENYI ZHANG*

School of Food Science and Technology, Jiangnan University, Wuxi 214122, Jiangsu Province, People's Republic of China

A delivery system for bioactive conjugated linoleic acid (CLA) through a self-assembled amylose−CLA complex was investigated in comparison with a β-cyclodextrin (BCD)−CLA complex. Successful complexation between CLA and amylose or BCD was confirmed by differential scanning calorimetry, X-ray diffraction, and Fourier transform infrared spectral analysis. The yield and complexing percentages were 71.9 and 1.4% for the amylose−CLA complex and 42.3 and 7.7% for the BCD−CLA complex, respectively. However, the amylose−CLA complex showed a better antioxidative protection effect on CLA than BCD−CLA complex, supporting a strong complexing interaction between CLA and amylose shown by thermogravimetric analysis. Compared to 15.9% of CLA released from the BCD−CLA complex under simulated small intestine conditions, 95.6% of CLA was released from the amylose−CLA complex. These results indicate that an amylose−lipid complex self-assembled in the natural way of food component interaction can be used to protect and deliver functional lipids or other bioactive components into the targeted small intestine for absorption.

KEYWORDS: Conjugated linoleic acid (CLA); amylose; β-cyclodextrin (BCD); self-assembled complex; targeted delivery

INTRODUCTION

Conjugated linoleic acid (CLA) is a collective term for a mixture of geometric and positional isomers of linoleic acid with a conjugated double bond starting from carbon 7, 8, 9, 10, or 11 (*1*). As a representive of polyunsaturated fatty acids (PUFA), it has been shown to have various health benefits, such as antidiabetes, antiadipogenesis, and anticarcinogenesis activities (*2*). Some clinical studies also showed positive results in reducing body fat mass (*3*, *4*) and increasing the resting metabolic rate without body weight changes(*5*). As obesity is a well-known risk factor to many metabolic diseases, reducing body fat through the consumption of CLA would decrease the incidence of these chronic diseases, and functional foods containing CLA would have a great potential to bring health benefits to consumers.

With the inherent structure of conjugated double bonds in CLA, which is highly susceptible to oxidative degradation leading to a loss of its bioactivity (*6*−*8*), there have been a number of studies focusing on improving the oxidative stability of CLA through physical or chemical methods. Green tea catechins (GTC) were shown to be effective as an antioxidant in protecting CLA from oxidation (*8*); polyethylene glycol (PEG) was reported to protect CLA from oxidation by covalent attachment of CLA to PEG (*9*); CLA microencapsulation using polymeric emulsifiers such as whey protein concentrate and gum arabic has also been reported (*10*, *11*) for food applications. Apparently, enrichment of bioactive CLA in foods represents an important research area in functional food, and the technical difficulties in delivering sufficient amounts of bioactive CLA through foods to have the desired physiological effects merit further exploration of novel delivery systems with superior properties in CLA-related functional food development.

The development of a protective delivery system for CLA based on the self-assembly property of soft matter is a newly emerged research area, and amylose and cyclodextrin are two classical examples. Amylose with a helical molecular structure can be self-assembled into an inclusion complex with many compounds, such as free fatty acids, through hydrophobic interaction (*12*, *13*), and the possibility of using this complex as a carrier for CLA has been reported (*14*). Cyclodextrin (CD), which is commonly used in food product development for various purposes, can also form an inclusion complex with hydrophobic molecules(*15*) through self-assembly, and a β-cyclodextrin (BCD)−CLA complex has also been reported for its antioxidative protection of CLA (*16*, *17*). However, most research results were focused on the in vitro oxidative stability, whereas research data on the delivery efficiency of CLA through these self-assembled complexes are scarce; additionally, few investigations have been done to compare the superiority between these two classical self-assembled delivery systems. Therefore, the antioxidative property and the targeted delivery of CLA using these two delivery systems were compared in this study, and it is expected this study will increase the knowledge pool of the self-assembly of soft food materials and their applications in delivering CLA or other functional compounds.

MATERIALS AND METHODS

Conjugated linoleic acid (O5507, a mixture of *cis*- and *trans*-9,11- and -10,12-octadecadienoic acids, linoleic acid < 1%),

*Corresponding author (e-mail genyiz@gmail.com).

Published on Web 07/02/2009

α-amylase (A3176, from porcine pancreas, EC 3.2.1.1), and pepsin (P7000, from porcine gastric mucosa, EC 3.4.23.1) were purchased from Sigma-Aldrich (Shanghai) Trading Co., Ltd. (Shanghai, China). Amyloglucosidase (EC 3.2.1.3) was obtained from Genencor (Wuxi) Bio-Products Pte Ltd. (Jiangsu, China). BCD (chemical pure) was from China National Medicines Corporation Ltd. (Shanghai, China). Amylose was isolated from potato starch using 1-butanol for selective precipitation(*18*).

Amylose−CLA Complex Preparation. Complexation of amylose with CLA was operated in a dimethyl sulfoxide (DMSO)/water solution (*14*). Briefly, amylose solution was prepared by dissolving amylose in DMSO (20 mg of amylose/mL of DMSO) at 90 °C and then was cooled to 30 °C. After dissolution of CLA in the amylose solution, distilled water at 30 °C was added, and the mixture was stirred for 15 min to form an amylose−CLA complex; NaCl solution (5%, w/v) was added to facilitate precipitation of the complex. The precipitated complex was separated by centrifugation and washed twice with ethanol (50%, v/v) to remove uncomplexed CLA. The complex was then vacuum-dried for further analysis. The yield of the complex was calculated according to the following formula: yield (%) = (mg of complex/mg of amylose and CLA) × 100.

BCD−CLA Complex Preparation. Complexation of BCD with CLA was carried out in ethanol/water solution (*16*). BCD was dispersed in distilled water and mixed with CLA (mole ratio of CLA/BCD was 1:1) in 95% ethanol solution. The mixture was stirred at 70 °C for 5 min and then cooled to room temperature for 4 h. After precipitation at 4 °C for 24 h, the precipitate was separated by vacuum filtration and washed by petroleum ether to remove uncomplexed CLA. The yield of the complex (%) was calculated in the same way as above.

Complexing Percentage Determination. Complexing percentage represents the amount of complexed CLA compared to the total amount of the complex, and its calculation was based upon sufficient extraction of CLA from the complexes. Amylose−CLA complex (15 mg) was incubated in 1 mL of enzyme solution (α-amylase, 200 units/mL; amyloglucosidase, 160 units/mL; $CaCl_2$, 0.01 mol/L; pH 5.2, 37 °C) until complete digestion of the complex, and the released CLA was extracted with hexane, followed by gas chromatography (GC) quantitative analysis (*14*). BCD−CLA complex (20 mg) was heated with distilled water (1 mL) and hexane (1.5 mL) in a small flask equipped with a condenser at 80 °C for 20 min with intermittent shaking. After cooling, the hexane layer containing CLA was separated and the aqueous layer was extracted with the same volume of hexane another three times. All of the CLA in the hexane layer was collected and then quantified. Complexing percentage = (mg of CLA released from complex/mg of the corresponding complex) × 100.

A GC instrument (Shimadzu GC-2010AF, Nanjing, China) equipped with a flame ionization detector (FID) and a CP-Wax 52 CB column (30 m length, 0.32 mm i.d. and 0.5 μm film thickness) was used to quantify the methyl ester of CLA. The temperature program was from 120 °C (maintained for 3 min) to 190 °C (maintained for 0.1 min) at a rate of 10 °C/min and then to 220 at 2 °C/min (maintained for 20 min). Both inlet and detector temperatures were 250 °C. The flow rates of nitrogen carrier gas, hydrogen combustion gas, combustion-supporting air, and nitrogen makeup gas were 3, 47, 400, and 30 mL/min, respectively. Peaks were identified by comparison with CLA standard from Sigma Chemical Co., and the methyl ester of CLA was quantified by using heptadecanoic acid as internal standard.

Differential Scanning Calorimetry (DSC). A Perkin-Elmer Pyris 1 DSC instrument (Perkin-Elmer Corp., Shanghai, China) was used to examine the thermal properties of the complexes. Amylose and amylose−CLA complex samples (5.0 mg) and distilled water (three times the weight of the solid) were sealed in aluminum pans to equilibrate overnight. The DSC scan was carried out from 30 to 150 °C at a rate of 5 °C/min. The DSC measurements of BCD and BCD−CLA complex samples (5.0 mg) were scanned from 30 to 200 °C at a heating rate of 4 °C/min.

X-ray Diffraction (XRD). A Bruker D8-Advance diffractometer (Bruker AXS Corp., Nanjing, China) equipped with Cu Kα radiation at 40 kV and 40 mA was used to obtain the X-ray diffractograms of the complexes. Amylose and amylose−CLA complex were scanned from 3° to 30° 2θ at a rate of 0.02°/3 s, whereas BCD and BCD−CLA complex were scanned from 2° to 45° 2θ at the same rate.

Fourier Transform Infrared Spectral (FTIR) Analysis. A Nicolet Nexus 470 Fourier transform infrared spectrometer (Thermo Electron Corp.) equipped with a DTGS detector and EZ Omnic (version 7.0) was used to obtain the spectrograms of the complexes. Accurately weighed samples and KBr (100 times the weight of each sample) were fully milled together and then squashed to get the infrared information by accumulating 32 scans per spectra at a resolution of 4 cm^{-1}.

Thermogravimetric Analysis (TGA). A Mettler Toledo TGA/SDTA851^e thermogravimeter (Mettler Toledo Corp., Zurich, Switzerland) with STAR^e software (version 9.01) was used to analyze the thermal stability of the complexes. Samples (2.0 mg in each 70 μL alumina pan) were heated from 50 to 400 °C (10 °C/min) under nitrogen gas flow (20 mL/min).

Antioxidation Test. The antioxidative protection effect of the complexes for CLA was evaluated by measuring peroxide values (POV) of CLA after the samples had been stored at 68 °C for different time periods. CLA (1.0−100.0 mg) was dissolved and diluted to 10 mL by chloroform/methanol (7:3, v/v) solution and mixed with ferrous chloride solution (0.05 mL, 3.5 mg/mL) and then potassium thiocyanate solution (0.05 mL, 300 mg/mL). The absorption was measured using a 722 grating spectrophotometer (Shanghai Precision and Scientific Instrument Corp., Shanghai, China) at 500 nm after at 5 min hold at room temperature. To make a standard curve for quantitative analysis, a series of iron standard solution was measured as above but without the addition of ferrous chloride solution. The POV was calculated according to the formula POV (mequiv/kg) = $(c - c_0)/(m \times 55.84 \times 2)$, where c and c_0 are the iron weight (μg) of the test sample and sample blank on the iron standard curve, respectively, m is the weight (g) of CLA in the test sample, 55.84 is the atomic weight of iron, and 2 is a converting factor. The iron standard solution (1 mg/mL) was prepared by dissolving reduced iron powder in hydrochloric acid and then diluted to 10.0 μg/mL using chloroform/methanol (7:3, v/v) solution. The POV of the CLA in the complexes was determined after ultrasonic extraction using chloroform/methanol (7:3, v/v) solution as solvent.

Release Test (A): Simulated Stomach Conditions. The release of CLA from the complexes in simulated stomach conditions was determined after the hydrolysis of amylose−CLA complex and BCD−CLA complex in simulated gastric juice. Complexes (15.0 mg) were incubated in 1.0 mL of HCl solution (pH 2.0) containing pepsin (5 mg/mL) at 37 °C under continuous shaking for 2 h. Then, CLA extracted with hexane from the mixture was analyzed by GC as described before. Release percentage = (weight of the released CLA/weight of the CLA in the corresponding complex) × 100.

Release Test (B): Simulated Small Intestine Conditions. The release of CLA from the complexes in simulated small intestine solution was measured following enzymatic digestion (α-amylase, 35 units/mL; amyloglucosidase, 35 units/mL; $CaCl_2$, 0.01 mol/L; pH 5.2) of amylose−CLA complex and BCD−CLA complex. Each complex had five parallel samples, and each sample contained 15.0 mg of complex. All of the samples were incubated in 1.0 mL of simulated small intestine solution at 37 °C under continuous shaking. An amylose−CLA complex sample and a BCD−CLA complex sample were taken out every 3 h; 0.2 mL was used to test the degree of enzyme digestion (using DNS method), and CLA in the residual hydrolysate was measured after extraction with hexane, followed by methylation and GC quantitative analysis as described before. Release percentage = (weight of the released CLA/weight of the CLA in the corresponding complex) × 100.

Data and Statistical Analysis. Experiments were carried out in duplicate for digestion tests and in triplicate for other tests, and results are presented as the average. Standard deviation was used to determine significant variability in quantitative analysis. OriginPro 8.0 (OriginLab Corp., Northampton, MA) was employed for statistical analysis.

RESULTS AND DISCUSSION

Self-Assembly of Amylose−CLA Complex. Amylose can form an inclusion complex with cis-unsaturated fatty acids in a self-assembled manner despite the nonlinearity of these fatty acids (*13*, *19*). All experimental data from DSC, XRD, and FTIR analyses showed that CLA, an unsaturated fatty acid including cis-isomerides, successfully complexed with amylose.

DSC is one of the common methods used to detect the formation of amylose−lipid complexes with a typical endothermic

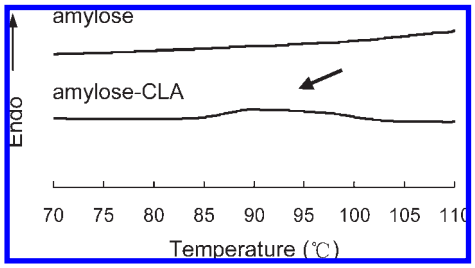

Figure 1. DSC thermograms of amylose and amylose−CLA complex.

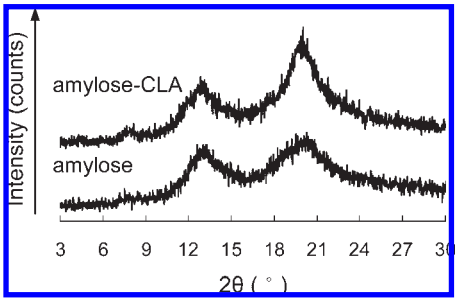

Figure 2. X-ray diffractograms of amylose and amylose−CLA complex.

peak around 100 °C. The DSC profile of the amylose−CLA complex showed an endothermic peak at 93 °C (**Figure 1**), indicating successful formation of the complex. The relatively lower endothermic peak temperature suggests the amylose−CLA complex belongs to a type I complex (*19*), which is in a metastable polymorph, and the additional double bonds in CLA might be the reason for the formation of this type I complex. The amylose−CLA complex with a lower dissociation temperature confirms the importance of the compatibility between the soft matter of amylose and its ligands in the process of self-assembly.

Self-assembly to form higher level structures between amylose and CLA is also supported by the typical V-pattern of XRD analysis (**Figure 2**). Amylose had two distinct peaks with similar intensities at $2\theta = 13.0°$ and 20.2°, whereas the amylose−CLA complex had three peaks with significantly increased intensities at $2\theta = 7.8°$, 12.9°, and 20.0°. Normally, potato amylose displays a B-type XRD pattern, whereas the amylose−lipid complex shows a V-pattern with a typical diffractive peak at 20.0° 2θ (*20*, *21*). However, from **Figure 2**, when the diffraction pattern of amylose−CLA complex was confirmed as a V-type one, that of amylose was also similar to V-type differing in the intensity of the diffraction peaks, but the diffractogram of the complex showed a better crystalline structure. The similar V-type diffraction pattern of amylose may be caused by the interaction of amylose with 1-butanol that was used for selective precipitation of amylose during its preparation.

Both DSC and XRD analyses confirmed the successful formation of amylose−CLA complex. To understand the driving force in the self-assembly process, FTIR was used to examine the differences among CLA, amylose, and amylose−CLA complex as shown in **Figures 3** and **4** and **Table 1**. The characteristic peaks of the functional groups of hydroxyl, carbonyl, and conjugated double bonds in CLA were found at 3435.02, 1712.19, and 1634.19 cm^{-1}, respectively. Compared with amylose, amylose−CLA complex showed a different infrared spectrogram: the basal part of the hydroxy peak broadened to much lower wavenumbers, and its peak near 1650.50 cm^{-1} became the strongest one (Figrue **4**, arrow). These changes indicate the existence of CLA in the amylose−CLA complex samples. In **Table 1**, similar hydroxyl peak positions (around 3422 cm^{-1}) of amylose, amylose−CLA

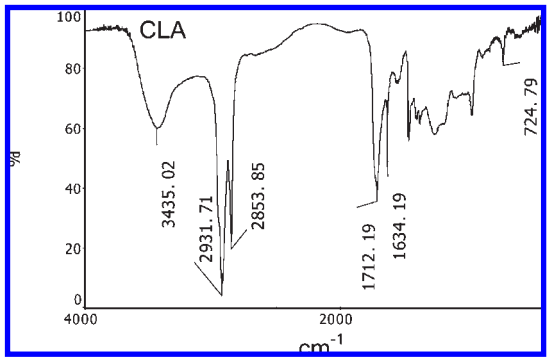

Figure 3. Infrared spectrogram of CLA.

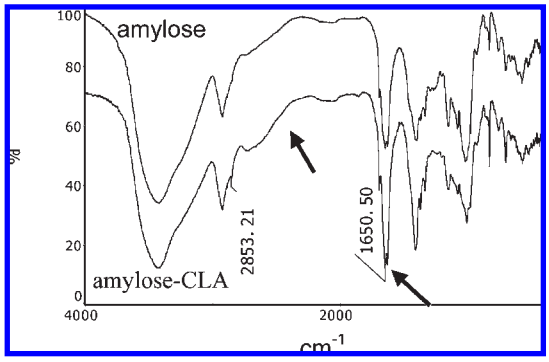

Figure 4. Infrared spectrograms of amylose and amylose−CLA complex.

Table 1. Hydroxy Peak Positions (cm^{-1}) of Amylose, BCD, and Their Complexes and Physical Mixings with CLA

material	material only	complex	physical mixing
amylose	3422.68 ± 1.84	3425.73 ± 1.82	3419.07 ± 2.59
BCD	3412.11 ± 4.58	3384.74 ± 0.43	3398.13 ± 2.12

complex, and physical mixing of amylose with CLA suggest that no noticeable hydrogen-bonding interaction exists between amylose and CLA, suggesting that the hydrophobic interaction, just like common amylose−lipid complexation, is the driving force for self-assembly between amylose and CLA.

Self-Assembly of BCD−CLA Complex. It is known that appropriate nonpolar molecules can displace the energetically unfavored water molecules in the BCD cavity to form an inclusion complex with BCD (*15*). All experimental data from DSC, XRD, and FTIR analyses showed that CLA, a nonpolar molecule, successfully complexed with BCD.

A small endothermic peak near 110 °C (**Figure 5**) from the DSC profile, which is distinctly different from the large and sharp peak around 180 °C caused by dehydration of BCD, indicates a successful formation of the self-assembled BCD−CLA complex, which is indirectly supported by literature data (*22*) that the complex between linoleic acid and α-cyclodextrin showed an endothermic peak near 120 °C. The formation of an inclusion complex between BCD and CLA is also supported by the partial crystalline structure from XRD analysis (**Figure 6**). BCD alone showed many sharp and narrow peaks prominently at $2\theta = 4.8°$ and 12.8°, whereas the BCD−CLA complex displayed a distinctly different XRD pattern with only one sharp and narrow peak at $2\theta = 11.8°$. Some early studies showed that BCD was a rather well-crystallized compound with many sharp peaks, and less crystalline structures will be formed when BCD forms complexes with other molecules (*23*−*25*), which is consistent with our results from the XRD analysis.

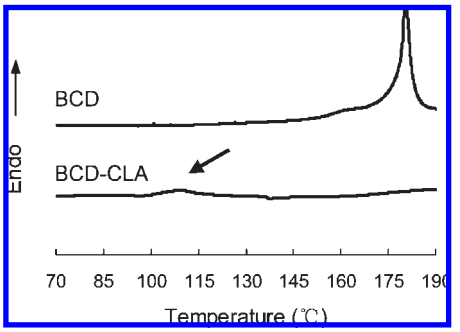

Figure 5. DSC thermograms of BCD and BCD−CLA complex.

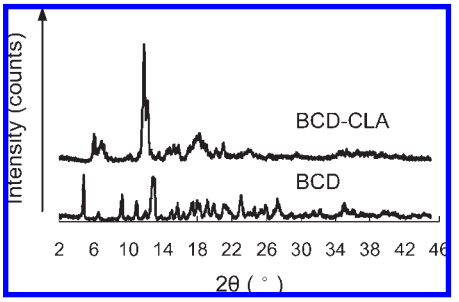

Figure 6. X-ray diffractograms of BCD and BCD−CLA complex.

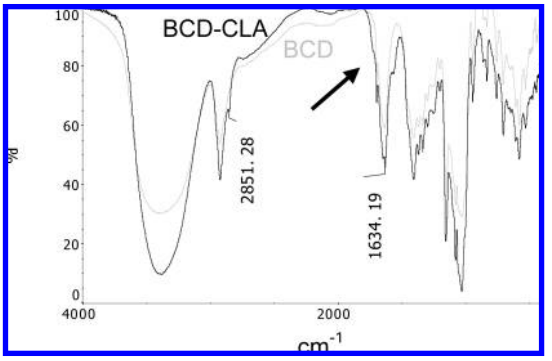

Figure 7. Infrared spectrograms of BCD and BCD−CLA complex.

Similarly, FTIR was used to examine the driving force in the self-assembly process between CLA and BCD, and the experimental results are shown in **Figures 3** and **7** and **Table 1**. Compared with CLA, the characteristic peaks of the functional groups in CLA could be found in the BCD−CLA complex, and, compared with BCD, the peak near 1634.19 cm^{-1} of the BCD−CLA complex broadened and strengthened (see the arrow). In **Table 1**, the hydroxyl peak position of the BCD−CLA complex is at least 26 cm^{-1} lower than that of BCD whereas the difference of this peak position between BCD and its physical mixing with CLA is not so distinct. This noticeable low shift of hydroxyl peak on the infrared spectrogram of the BCD−CLA complex suggests that hydrogen-bonding interaction is one of the driving forces for self-assembly between BCD and CLA except the well-known hydrophobic interaction between BCD and nonpolar molecules.

Thermal Stability of Amylose−CLA and BCD−CLA Complexes. Differences in thermal stability among CLA, amylose, and amylose−CLA complex were examined by thermogravimetric analysis shown in **Figure 8**. Each of the samples showed only a steep step of weight loss caused by their thermal decomposition in the thermogravimetric curves, and the initial weight loss temperatures for CLA, amylose, and amylose−CLA complex were 146.69, 269.18, and 240.60 °C, respectively. A one-step

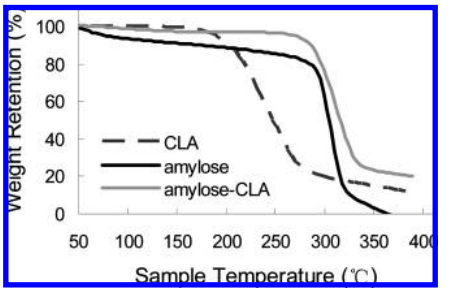

Figure 8. Thermogravimetric curves of CLA, amylose, and amylose−CLA complex.

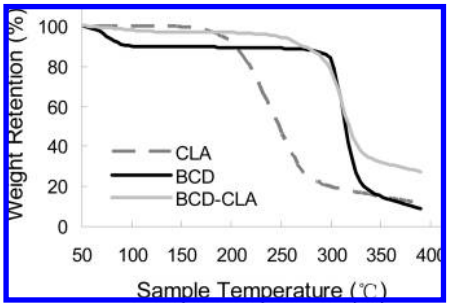

Figure 9. Thermogravimetric curves of CLA, BCD, and BCD−CLA complex.

Table 2. Yield and Complexing Percentage of the Complexes

complex	yield (%)	complexing percentage
amylose−CLA	71.95 ± 6.29	1.39 ± 0.31
BCD−CLA	42.25 ± 0.49	7.67 ± 0.58

thermogravimetric curve of the amylose−CLA complex indicates the complex is decomposed as one unified structure suggesting a strong interaction between amylose and CLA in the complex, which is different from a physical blend of different compounds with the same step number as its component number.

Differences in thermal stability among CLA, BCD, and BCD−CLA complex are also shown by TGA in **Figure 9**. Both of the thermogravimetric curves of BCD and BCD−CLA complex had two distinct steps, and the initial weight loss temperatures of the two steps for BCD were 50.79 and 275.80 °C and those for BCD−CLA were 245.97 and 274.82 °C, respectively. For BCD, the first stage of weight loss is caused by dehydration of BCD molecules, and the second one is caused by thermal decomposition of BCD. For the BCD−CLA complex, the first small stage of weight loss corresponds to the loss of CLA in the BCD cavity, and the second one is caused by thermal decomposition of BCD. Apparently, the self-assembled formation of the BCD−CLA complex is supported by the disappearance of the noticeable dehydration stage and the appearance of a small stage in a temperature lower than the BCD decomposition temperature. On the other hand, a two-step weight loss in the thermal decomposition of the BCD−CLA complex suggests that self-assembly between BCD and CLA is not so strong as that of amylose and CLA with a single-step weight loss.

Self-Assembled Efficiency and Antioxidative Effect. To compare the complexation efficiency of the two complexes, their yields and complexing percentages were measured, and the results are shown in **Table 2**. Compared with the BCD−CLA complex, the yield of the amylose−CLA complex was higher, but its complexing percentage was much lower. This disadvantage of the amylose−CLA complex might be caused by the conjugated

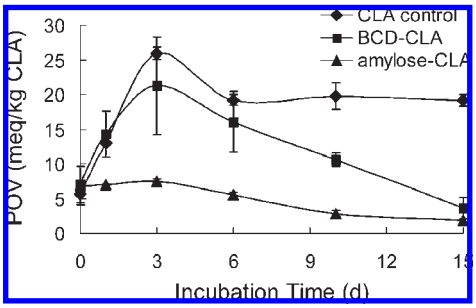

Figure 10. POV changes of CLA with incubation time at 68 °C. CLA control is free CLA used in complex preparation, and BCD−CLA complex and amylose−CLA complex stand for CLA extracted from the corresponding complex.

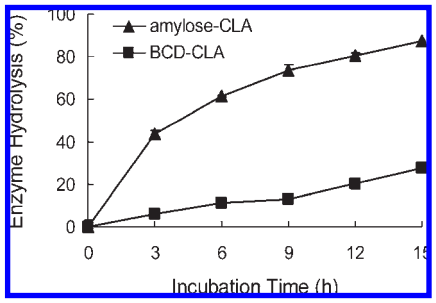

Figure 11. Changes of enzymolysis extent (%) in the simulated small intestine conditions during 15 h. Samples were hydrolyzed by both α-amylase and amyloglucosidase at concentrations of 35 units/mL. The influence of control without complexes was considered.

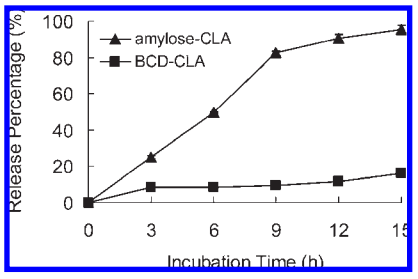

Figure 12. Release percentage of the complexes in the simulated small intestine conditions during 15 h.

double bonds in CLA that is likely a steric hindrance for a high ratio of complexation between CLA and amylose.

However, the antioxidative protection effect of the amylose−CLA complex showed better performance than the BCD−CLA complex (**Figure 10**). During the first 3 days of storage, the POVs of both the control and CLA extracted from BCD−CLA complex increased rapidly, but the POVs of CLA extracted from amylose−CLA complex were almost unchanged. After 3 days, the POVs of all of the samples decreased due to depletion of peroxides after reaching a high concentration, and the slowest changes of POV for CLA from amylose−CLA complex further showed its protective effect on the complexed CLA.

There have been studies showing that starch (mainly amylose) can interact with lipid to form complexes that have antioxidative capability and high thermal stability (*26*, *27*), which is consistent with our result of the single-step thermogravimetric curve of the amylose−CLA complex (**Figure 8**), indicating that the strong interaction between CLA and amylose would limit oxygen accessibility and decrease CLA oxidation. Comparatively, a lower antioxidative protection effect of BCD−CLA complex was shown by its CLA POVs, which increased first and then decreased to a higher POV value than that from the amylose−CLA complex. Possibly, these POV changes suggest that the protection provided by BCD for CLA has different degrees, and this uneven protection effect likely results from a weak interaction between BCD and CLA in the complex with a two-step thermogravimetric curve. Thus, the tightness of interaction between CLA and its carrier possibly determines the oxidative protection effect on CLA.

Targeted Delivery Effect. The release percentages in the simulated stomach and small intestine conditions were examined to evaluate the stability of the complexes under the gastrointestinal conditions. A high release percentage (11.49 ± 0.78%) was observed for BCD−CLA complex during 2 h of incubation in the simulated stomach conditions, whereas no CLA could be detected in amylose−CLA complex samples. As shown in **Figures 11** and **12**, both the extents of enzyme hydrolysis and the release percentages of the complexes increased during the 15 h of incubation in the simulated small intestine conditions, but the speed and extent of the increase for the two complexes were quite different. The enzyme hydrolysis extent and release percentage for the amylose−CLA complex rose gradually to 87.50 and 95.61%, but for the BCD−CLA complex these increased to only 27.92% and 15.96%, respectively. These results indicate that most of the amylose−CLA complex has been digested and almost all of the complexed CLA was released, which would lead to an improved bioavailability of CLA. In contrast, the BCD−CLA complex is not so efficient for CLA utilization.

The high stability of the amylose−CLA complex in the simulated stomach conditions is likely caused by the acid insolubility of amylose and the strong interaction between amylose and CLA as well as the complexation method as reported (*14*). Although the susceptibility of amylose to α-amylase hydrolysis is reduced by its interaction with CLA, the CLA can still be adequately released in the simulated small intestine conditions as the digestion of amylose by corporate action of α-amylase and amyloglucosidase. Therefore, the amylose−CLA complex could be used as a targeted delivery system for CLA to maintain its antioxidative stability with efficient targeted release property.

The BCD−CLA complex is less stable than the amylose−CLA complex in the simulated stomach conditions due to the acid instability of BCD and the weak interaction between CLA and BCD in the complex. However, in the simulated small intestine conditions, the poor solubility of BCD and its inherent resistance to enzyme action would result in a less release of CLA and so its bioavailability. Therefore, the BCD−CLA complex is not an efficient delivery system for CLA from the perspective of stability and targeted delivery.

It should be noted that the enzyme concentration (35 units/mL) used to simulate the small intestine conditions is regarded as the minimal activity in the intestine (*14*), and a 15 h hydrolysis time seems much longer than the real digestion time in small intestine. However, a 15 h in vitro incubation with α-amylase and amyloglucosidase was shown to correspond well to the amount of starch escaping digestion in human small intestine (*28*), and the experimental results for complexes of amylose−CLA and BCD−CLA suggest the chosen conditions are valid for the purpose of comparing the differences between the complexes for targeted CLA delivery. It is expected that the amylose−CLA complex will be completely digested under normal small intestine conditions with much higher enzyme concentration.

Efficient Self-Assembled Delivery System. An efficient delivery system for CLA should protect CLA from oxidation and carry it to the destination of small intestine with minimal loss in other parts of the gastrointestinal tract. Considering the efficiency of targeted delivery, the amylose−CLA complex can serve as a

better vehicle for CLA delivery than the BCD−CLA complex, although both of them prepared in appropriate conditions can adequately protect CLA from oxidation (*14*, *17*). Besides, the amylose−CLA complex is self-assembled through natural food component interaction, which does not need specific processing steps in functional food applications. However, the low complexing percentage and insolubility of the amylose−CLA complex would become obstacles for its practical use, so further work should be done to solve these two problems. Gunaratne's study showed the influence of BCD on amylose−lipid complex(*29*), and the complexing percentage of BCD−CLA complex is much higher than that of amylose−CLA complex, so self-assembled interaction among amylose, BCD, and CLA may occur to improve the complexing percentage and maintain the antioxidative stability and targeted delivery property. Additionally, substituting an amylose−CLA−protein complex for the amylose−CLA complex might solve its insolubility problem because a novel self-assembled complex consisting of starch, protein, and free fatty acids has been found to be water-soluble (*30*, *31*).

LITERATURE CITED

(1) Park, Y.; Pariza, M. W. Mechanisms of body fat modulation by conjugated linoleic acid (CLA). *Food Res. Int.* **2007**, *40*, 311–323.

(2) Bhattacharya, A.; Banu, J.; Rahman, M.; Causey, J.; Fernandes, G. Biological effects of conjugated linoleic acids in health and disease. *J. Nutr. Biochem.* **2006**, *17*, 789–810.

(3) Blankson, H.; Stakkestad, J. A.; Fagertun, H.; Thom, E.; Wadstein, J.; Gudmundsen, O. Conjugated linoleic acid reduces body fat mass in overweight and obese humans. *J. Nutr.* **2000**, *130*, 2943–2948.

(4) Thom, E.; Wadstein, J.; Gudmundsen, O. Conjugated linoleic acid reduces body fat in healthy exercising humans. *J. Int. Med. Res.* **2001**, *29*, 392–396.

(5) Kamphuis, M.; Lejeune, M.; Saris, W. H. M.; Westerterp-Plantenga, M. S. The effect of conjugated linoleic acid supplementation after weight loss on body weight regain, body composition, and resting metabolic rate in overweight subjects. *Int. J. Obesity* **2003**, *27*, 840–847.

(6) Yurawecz, M. P.; Hood, J. K.; Mossoba, M. M.; Roach, J. A. G.; Yu, Y. Furan fatty acids determined as oxidation products of conjugated actadecadienoic acid. *Lipids* **1995**, *30*, 595–598.

(7) Zhang, A.; Chen, Z. Y. Oxidative stability of conjugated linoleic acids relative to other polyunsaturated fatty acids. *J. Am. Oil Chem. Soc.* **1997**, *74*, 1611–1613.

(8) Yang, L.; Leung, L. K.; Huang, Y.; Chen, Z. Y. Oxidative stability of conjugated linoleic acid isomers. *J. Agric. Food Chem.* **2000**, *48*, 3072–3076.

(9) Moon, H. S.; Lee, H. G.; Seo, J. H.; Chung, C. S.; Kim, T. G.; Kim, I. Y.; Lim, K. W.; Seo, S. J.; Choi, Y. J.; Cho, C. S. Down-regulation of PPAR gamma 2-induced adipogenesis by PEGylated conjugated linoleic acid as the pro-drug: attenuation of lipid accumulation and reduction of apoptosis. *Arch. Biochem. Biophys.* **2006**, *456*, 19–29.

(10) Jimenez, M.; Garcia, H. S.; Beristain, C. I. Spray-drying microencapsulation and oxidative stability of conjugated linoleic acid. *Eur. Food Res. Technol.* **2004**, *219*, 588–592.

(11) Jimenez, M.; Garcia, H. S.; Beristain, C. I. Spray-dried encapsulation of conjugated linoleic acid (CLA) with polymeric matrices. *J. Sci. Food Agric.* **2006**, *86*, 2431–2437.

(12) Polaczek, E.; Starzyk, F.; Maleńki, K.; Tomasik, P. Inclusion complexes of starches with hydrocarbons. *Carbohydr. Polym.* **2000**, *43*, 291–297.

(13) Karkalas, J.; Raphaelides, S. Quantitative aspects of amylose−lipid interactions. *Carbohydr. Res.* **1986**, *157*, 215–234.

(14) Lalush, I.; Bar, H.; Zakaria, I.; Eichler, S.; Shimoni, E. Utilization of amylose−lipid complexes as molecular nanocapsules for conjugated linoleic acid. *Biomacromolecules* **2005**, *6*, 121–130.

(15) Szejtli, J. Introduction and general overview of cyclodextrin chemistry. *Chem. Rev.* **1998**, *98*, 1743–1753.

(16) Park, C. W.; Kim, S. J.; Park, S. J.; Kim, J. H.; Kim, J. K.; Park, G. B.; Kim, J. O.; Ha, Y. L. Inclusion complex of conjugated linoleic acid (CLA) with cyclodextrins. *J. Agric. Food Chem.* **2002**, *50*, 2977–2983.

(17) Kim, S. J.; Park, G. B.; Kang, C. B.; Park, S. D.; Jung, M. Y.; Kim, J. O.; Ha, Y. L. Improvement of oxidative stability of conjugated linoleic acid (CLA) by microencapsulation in cyclodextrins. *J. Agric. Food Chem.* **2000**, *48*, 3922–3929.

(18) Gilbert, L. M.; Gilbert, G. A.; Spragg, S. P. Amylose and amylopectin from potato starch. In *Methods in Carbohydrate Chemistry, Starch*; Whistler, R. L., Ed.; Academic Press: New York, 1964; Vol. *IV*, pp 25−27.

(19) Karkalas, J.; Ma, S.; Morrison, W. R.; Pethrick, R. A. Some factors determining the thermal properties of amylose inclusion complexes with fatty acids. *Carbohydr. Res.* **1995**, *268*, 233–247.

(20) Gelders, G. G.; Vanderstukken, T. C.; Goesaert, H.; Delcour, J. A. Amylose−lipid complexation: a new fractionation method. *Carbohydr. Polym.* **2004**, *56*, 447–458.

(21) Godet, M. C.; Bizot, H.; Buléon, A. Crystallization of amylose-fatty acid complexes prepared with different amylose chain lengths. *Carbohydr. Polym.* **1995**, *27*, 47–52.

(22) Tatsuji, I.; Shuji, A.; Ryuichi, M. Thermogravimetric analysis of cyclodextrin−fatty acid complex formation and its use for predicting suppressed autoxidation of fatty-acids. *Biosci., Biotechnol., Biochem.* **1995**, *59*, 51–54.

(23) Zhang, A.; Liu, W.; Wang, L.; Wen, Y. Characterization of inclusion complexation between fenoxaprop-*p*-ethyl and cyclodextrin. *J. Agric. Food Chem.* **2005**, *53*, 7193–7197.

(24) Villavede, J.; Morillo, E.; Pérez-Martínez, J. I.; Ginés, J. M.; Maqueda, C. Preparation and characterization of inclusion complex of norflurazon and β-cyclodextrin to improve herbicide formulations. *J. Agric. Food Chem.* **2004**, *52*, 864–869.

(25) Caccia, F.; Dispenza, R.; Fronza, G.; Fuganti, C.; Malpezzi, L.; Mele, A. Structure of neohesperidin dihydrochalcone/β-cyclodextrin inclusion complex: NMR, MS, and X-ray spectroscopic investigation. *J. Agric. Food Chem.* **1998**, *46*, 1500–1505.

(26) Morrison, W. R.; Mann, L. D. Selective extraction and quantitative analysis of non-starch and starch lipids from wheat flour. *J. Sci. Food Agric.* **1975**, *26*, 207–521.

(27) Morrison, W. R. The stability of wheat starch lipids in untreated and chlorine-treated cake flours. *J. Sci. Food Agric.* **1978**, *29*, 365–371.

(28) Muir, J. G.; O'Dea, K. Validation of an in vitro assay for predicting the amount of starch that escapes digestion in the small intestine of humans. *Am. J. Clin. Nutr.* **1993**, *57*, 540–546.

(29) Gunaratne, A.; Corke, H. Influence of unmodified and modified cycloheptaamylose (β-cyclodextrin) on transition parameters of amylose−lipid complex and functional properties of starch. *Carbohydr. Polym.* **2007**, *68*, 226–234.

(30) Zhang, G.; Hamaker, B. R. Detection of a novel three component complex consisting of starch, protein, and free fatty acds. *J. Agric. Food Chem.* **2003**, *51*, 2801–2805.

(31) Zhang, G.; Hamaker, B. R. A three component interaction among starch, protein, and free fatty acids revealed by pasting profiles. *J. Agric. Food Chem.* **2003**, *51*, 2797–2800.

Received May 15, 2009. Revised manuscript received June 17, 2009. Accepted June 19, 2009. This research work is supported by the National Natural Science Foundation of China (20676054), PCSIRT0627, and 111 project-B07029.